Infrared Physics & Technology 137 (2024) 105116

Contents lists available at ScienceDirect

Infrared Physics and Technology

journal homepage: www.elsevier.com/locate/infrared

Compensation of composition variation-induced sensitivity changes in gas phase photoacoustics

Panna Végh [a,*], Gábor Gulyás [a], Helga Huszár [a,b], Tibor Ajtai [a], Gábor Szabó [a], Anna Szabó [a,b], Zoltán Bozóki [a,b]

[a] Department of Optics and Quantum Electronics, University of Szeged, Dóm tér 9, H-6720 Szeged, Hungary
[b] ELKH-SZTE Research Group for Photoacoustic Monitoring of Environmental Processes, Dóm tér 9, H-6720 Szeged, Hungary

ARTICLE INFO

Keywords:
Gas phase
Photoacoustics
Heat capacity ratio
Novel calibration methodology

ABSTRACT

Infrared photoacoustic (PA) spectroscopy is a widely used technique to monitor trace gas concentration changes during industrial processes where the bulk composition may vary considerably. However, the PA signal is prone to changes in bulk composition, leading to relative uncertainties in measurements of up to 10%, due to the complex dependence of the sensitivity of a PA system (S) on the thermal and acoustic properties of the gas sample. A novel calibration and concentration calculation method is proposed to keep the relative accuracy of the PA measurements in the few percentages range even in case of large-scale composition variations. The main novelty of the proposed method is that it tackles the complex dependence of the PA system's sensitivity in a way that while it varies the resonance frequency of the calibration gas, it keeps the heat capacity ratio of calibration gases at a constant value. We prove that it determines the analyte's concentration with relative accuracy of about 1 %, even when the composition of the gas varies drastically. It rigorously compensates for the frequency and heat capacity ratio dependence of S and for the dependence of the half-width of the resonance curve of the PA cell on the thermal and acoustic properties of the gas. Although the reported demonstration measurements are executed in a relatively simple gas mixture, the proposed method has widespread applicability in high-precision monitoring.

1. Introduction

Photoacoustic (PA) concentration measurement technique has a well-established reputation for being a highly selective, sensitive, and accurate concentration measurement technique. Early PA measurements [1] have already proven these advantages and initiated a continuous increase in the use of the PA technique in various applications, including exhaled breath analysis [2,3], industrial process monitoring and control [4,5], environmental monitoring [6], miniaturized sensors [7,8], etc. The attractiveness of the method partially stems from an apparently very simple expression for the sensitivity of a PA system [9,10]:

$$S = (\gamma - 1)\cdot C\cdot P_{\mathrm{in}}\cdot\alpha_{\mathrm{spec}} \tag{1}$$

In Equation (1), the sensitivity (S in V/ppm) is defined as the PA signal generated by the unit concentration of the measured analyte, γ is the heat capacity ratio of the measured gas, C is the so-called cell constant (in $\mathrm{V\cdot cm\cdot W^{-1}}$), P_{in} is the light power of the laser beam entering the PA cell (in W), and α_{spec} is the specific optical absorption coefficient of the unit concentration of the light absorbing component (in $\mathrm{cm^{-1}\cdot ppm^{-1}}$). Although Equation (1) neglects several effects such as spectral interference, the effect of noninstantaneous molecular relaxation, the presence of background PA signal generated by light absorption on the walls and windows of the PA cell, these effects can be handled either by proper selection of the measurement wavelength and by using various algorithms:

- Locking the laser wavelength and the laser modulation frequency to the selected optical absorption feature [11] and to the top of the selected acoustic resonance curve [12], respectively,
- Compensating pressure and temperature dependencies [13,14], background PA signal variations [15], and the effects of non-instantaneous nonradiative relaxation processes [16,17],

* Corresponding author at: Department of Optics and Quantum Electronics, University of Szeged, Dóm tér 9, H-6720 Szeged, Hungary.
E-mail address: vegh.panna@szte.hu (P. Végh).

https://doi.org/10.1016/j.infrared.2023.105116
Received 4 August 2023; Received in revised form 25 October 2023; Accepted 30 December 2023
Available online 4 January 2024

- Executing multicomponent analysis in order to suppress the effects of spectral interference from the gas matrix [18].

With these self-checking and self-correcting methods, the relative accuracy of the PA measurement can be kept in the low percentage range, at least in the case of measuring in gases with stable concentration of its main components. However, as soon as the composition of the measured gas begins to vary it turns out that while Equation (1) is fundamentally valid, it must be written in another form that contains all the dependencies of the PA system's sensitivity on the material properties of the measured gas:

$$S(f,(\gamma-1)) = \frac{(\gamma-1)}{\Delta f(f,(\gamma-1))} \cdot M(f) \cdot \frac{\int p(r)\cdot I(r)\,dV}{A\cdot\pi^2} \cdot P_{\text{in}} \cdot \alpha_{\text{spec}} \tag{2}$$

In Equation (2), f is the gas composition-dependent resonance frequency of the PA cell (in Hz), meaning that the laser modulation frequency is assumed to be kept continuously at the top of the acoustic resonance curve whenever it changes due to composition change. Furthermore, Δf is the full width at half maximum (FWHM) of the acoustic resonance of the PA cell (in Hz), M is the frequency dependent sensitivity of the measuring microphone (in $mV \bullet Pa^{-1}$), A is the cross-section of the PA resonator (in m^2). Furthermore, the overlap integral ($\int p(r)\cdot I(r)dV$) accounts for the fact that depending on the spatial distribution of the pressure and the laser intensity [$p(r)$ and $I(r)$], respectively, acoustic resonances within the PA cell can be excited with varying efficiency. The geometry of the PA cell used in this study (the longitudinal differential cell) is optimized in a way to yield a high numerical value of the overlap integral whenever the laser modulation frequency is equal to the resonance frequency of the first longitudinal acoustic resonance. Both the microphone's sensitivity and the FWHM of the acoustic resonance have frequency dependence as indicated by the notation. However, acoustic losses also depend on the thermal properties of the measured gas [19], causing an indirect dependency of S on the (γ-1) parameter too, complementing the well-known direct proportionality between S and (γ-1). Fig. 1 visualizes these complex interdependencies.

To illustrate the scale of changes in the PA system's sensitivity generated by gas composition variations one can take an example from the oil and gas industry, where analytical instruments are routinely applied for measuring the concentration of pollutants (such as hydrogen-sulfide, water vapor and carbon-dioxide) of gas streams at ppm levels [4]. These instruments are often deployed at operational sites where the measured gas periodically alternates between heavy hydrocarbon mixtures and hydrogen-rich samples, and consequently the sound speed of the measured gas varies from 150 to 800 m/s [20]. Whereas the resonance frequency of a PA cell is proportional to the sound speed, therefore, the resonance frequency of a longitudinal differential PA cell measuring this gas stream changes from 2 kHz to 10 kHz. Over this frequency range the cell constant varies by about a factor of four. Even greater changes in sensitivity can be attributed to the variation in the (γ-1) value as it is about 0.1 and 0.6 for a hydrogen-rich and for a heavy component rich sample, respectively [21]. A second, albeit less dramatic, example is capnography, i.e. measurement of components in exhaled air, where within a single expiratory cycle, carbon dioxide (CO_2) concentration changes from 0 to about 5 % [22].

Several studies have concentrated on the effects of gas composition variations on the accuracy of the PA measurements [16,20,23–26]. Recently, Guo et al. effectively enhanced the acoustic resonance amplification performance of their PA cell by taking advantage of the physical parameters of the background gas [27]. Compared to nitrogen the physical properties of sulfur hexafluoride (SF_6) background gas significantly improved the quality factor of their PA cell. The drastic effects of gas composition variations on the PA signal were theoretically studied by Rück et al. [26]. They fully analytically computed the PA signal by simulation of γ and energy transfer processes, while the ratio of the quality factor and the resonance frequency was continuously measured. As a result, a Digital Twin of a photoacoustic trace gas sensor for methane was created and evaluated regarding variations in gas composition, pressure and temperature.

The aim of this paper is to study the effects of gas composition variation empirically and to propose a procedure for the compensation of sensitivity changes. The paper is organized as follows. Section 2 describes the proposed method. Section 3 presents the experimental setup used to demonstrate the outstanding accuracy achievable with the proposed method. Section 4 presents the results. Section 5 discusses several aspects of the presented work, while Section 6 summarizes the conclusions.

2. Theoretical and experimental considerations of the proposed method

The fundamental novelty of the proposed method is that it addresses

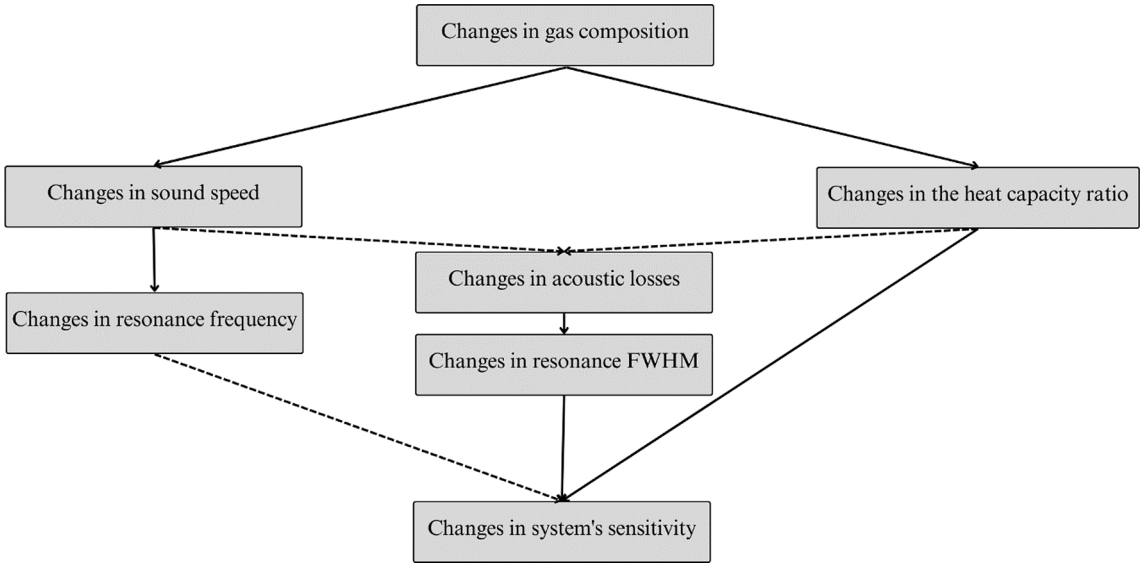

Fig. 1. Graphical representation of the cascade of changes induced by gas composition variations leading to the composition dependency of the sensitivity of a PA system. Dependencies that can be calculated with simple mathematical formulas or can be determined via measurements only are represented by solid and dashed arrows, respectively. (See text for further details.).

the complex dependence of the PA system's sensitivity in a way that while it varies the resonance frequency of the PA cell, it keeps the heat capacity ratio of the calibration gases constant. For simplicity, in the following S (f,(γ-1)) and Δf (f,(γ-1)) are marked with S (f) and Δf (f), respectively. Besides, the subscripts c and a correspond to those values at which the calibrations and actual measurements are executed, respectively.

2.1. Calibration with gas mixtures having constant γ

Here we suggest to execute calibrations with a set of calibration gas mixtures characterized by the same heat capacity ratio. This can be implemented by adding mixtures of a heavy and a light noble gas to the initial gas in a way that the individual concentrations of the noble gases are varied but their total concentration is kept constant. In this way, sensitivity changes induced by resonance frequency variations can be separated from changes induced by heat capacity ratio variations. The value of the heat capacity ratio during calibration, the deduced sensitivities and resonance FWHMs are marked in the following as $(\gamma\text{-}1)_c$, S_c (f_c) and Δf_c (f_c), respectively. Here f_c corresponds to those frequencies at which the calibrations are executed. There are several other requirements for the calibrations:

- The initial gas or gas mixture should resemble the typical composition for subsequent applications as much as possible.
- Each calibration should be executed by adding various amounts of the targeted analyte to the gas mixture in a way that the concentrations of the main gas components remain constant. The simplest way for that is using two gas cylinders, one containing the measured analyte buffered in a carrier gas, another containing the carrier gas only. Whenever the volumetric flows from the two cylinders are varied, but their total flow is kept constant, the analyte concentration can be varied without changing the concentration of the carrier gas component in the total gas mixture.
- The frequency range of the calibrations should cover the expected range of the subsequent application. This range can be tailored via the proper selection of the ratio of the concentrations of the two noble gases to cover the entire frequency range expected to occur during subsequent applications.

The numerical values of S_c (f_c) and Δf_c (f_c) at the given carrier gas composition (i.e., at the pre-selected resonance frequencies) can be determined as the slope of the line fitted to the PA signal (f_c) − c data points, and as a fitting parameter of the Lorentzian curve fitted to the resonance curve measured at the highest analyte concentration, respectively.

Finally, after completing the calibration measurements at the selected frequencies, the frequency dependence of the sensitivity and of the FWHM can be estimated for the targeted frequency range by fitting interpolation curves to the measured S_c (f_c) and Δf_c (f_c) data points. With these parameters the PA system is ready for use during the actual concentration measurements as described next. The steps of the method are shown in Fig. 2 (and in Table 1).

2.2. Concentration calculation

Precise concentration measurements in gas mixtures with varying gas composition has to be supplemented with measurements of the actual value of (γ-1) and the FWHM marked as $(\gamma\text{-}1)_a$ and Δf (f_a), respectively. (For the tests reported here, these actual values are listed in Table 2.) With all these data and with the interpolated calibration curves, the sensitivity of the PA system can be derived by using the following equation:

$$S_a\,(f_a) = S_c\,(f_a)\cdot\frac{(\gamma-1)_a}{(\gamma-1)_c}\cdot\frac{\Delta f_c\,(f_a)}{\Delta f_a\,(f_a)} \tag{3}$$

where S_a (f_a) is the estimation of the actual sensitivity at the actual resonance frequency (f_a) and gas composition, while S_c (f_a) and Δf_c (f_a) are the sensitivity and FWHM, respectively, determined during calibration and interpolated to f_a.

Equation (3) is the result of a simple algebraic rearrangement of Equation (2) in a way that it is written for both the calibration and the measurement, then in both cases all non-varying factors, including P_{in}, α_{spec}, A, the overlap integral etc. are rearranged on the right-hand side of the two equations. The equity of the left-hand sides of the two rearranged equations leads to Equation (3).

Once the calculation of the S_a (f_a) value by Equation (3) is completed, the actual analyte concentration can be deduced by subtracting the background signal from the measured PA signal and by dividing the result with S_a (f_a) (see Equation (2).

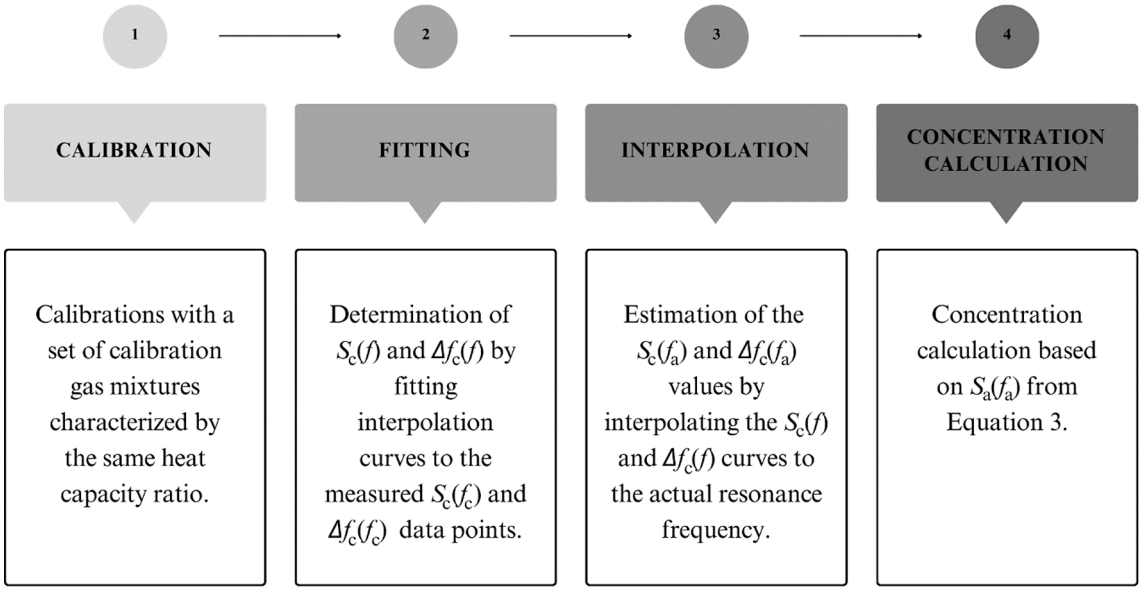

Fig. 2. Graphical representation of the steps of the proposed calibration and concentration calculation procedure to compensate the composition dependency of the sensitivity of a PA system.

2.3. Supplementary considerations

The amount of noble gas mixture added to the initial gas or gas mixture must be optimized. On the one hand, too high concentrations of the noble gas mixture would lead to too low analyte concentrations, which in turn would result in a poor signal to noise ratio of the measurement, resulting in high inaccuracy of the determined S_c (f_c) and Δf_c (f_c) parameters. On the other hand, low noble gas concentration allows for the determination of the frequency dependences of the sensitivity and the FWHM in a narrow frequency range only.

The preliminary planning of the frequency range of the calibration can be based on the following estimation of the resonance frequency of a longitudinal PA cell [9]:

$$f_0 = \frac{1}{2\,(L+0.6r)}\sqrt{\frac{\frac{c_p}{c_v}\cdot R\cdot T}{M}} \tag{4}$$

where L and r are the length and the radius of the resonator (in m), respectively, R is the ideal gas constant (in $J\cdot mol^{-1}\cdot K^{-1}$), M is the molar mass of the gas mixture (in $kg\cdot mol^{-1}$) and T is temperature of the PA cell (in the current case it was 313 K). The molar mass of the gas mixture can be determined by the weighted average of the molar masses of each component [21]:

$$M = \sum_i y_i \cdot M_i \tag{5}$$

where y_i is the molar fraction and M_i is the molar mass of component i. The molar heat capacity at constant pressure of the ideal gas mixture can be obtained by [21]

$$c_p = \sum_i y_i \cdot c_{p_i} \tag{6}$$

where y_i is the molar fraction of component i in the gas mixture and c_{p_i} is the molar heat capacity of the same component at flowing temperature. Equations (5) and (6) consider all components of the gas matrix, including the target analyte. However, in case its concentration does not exceed the percentage level, it can be neglected. The heat capacity of the components at constant pressure at 313 K can be determined using a calculation method based on polynomial factors [28]. Knowing the molar heat capacity of the gas components at constant pressure, the (γ-1) value of the gas mixture can be given as

$$\gamma - 1 = \frac{\sum_i y_i \cdot c_{p_i}}{\sum_i y_i \cdot c_{p_i} - R} - 1 \tag{7}$$

The estimated values of the resonance frequencies and the calculated heat capacity ratios are listed in Tables 1 and 2 (see below).

Next, experimental details of the first testing of the proposed measurement method are given.

Table 1
Gas compositions used during the calibration of the PA system.

Volumetric mixing ratios			$(\gamma-1)_c$	Resonance frequency (Hz)	Resonance frequency (Hz)
CH_4	Ar	He	(calculated)	(estimated)	(measured)
0.250	0.750	0.000	0.509	4380	4421
0.250	0.550	0.200	0.509	4933	4974
0.250	0.410	0.340	0.509	5474	5524
0.250	0.305	0.445	0.509	6022	6084
0.250	0.220	0.530	0.509	6610	6684
0.250	0.160	0.590	0.509	7148	7224
0.250	0.105	0.645	0.509	7776	7863

Table 2
Gas compositions used during the test of the proposed method. To simplify their subsequent identification, the calibrations are numbered sequentially.

Sequential number	Volumetric mixing ratios			$(\gamma-1)_c$	Resonance frequency (Hz)	Resonance frequency (Hz)
	CH_4	Ar	He	(calculated)	(estimated)	(measured)
1.	0.40	0.60	0.00	0.446	4533	4483
2.	0.50	0.25	0.25	0.412	5666	5687
3.	0.60	0.40	0.00	0.383	7300	7278
4.	0.70	0.14	0.16	0.358	5739	5808
5.	0.90	0.05	0.05	0.318	5849	5854

3. Experimental section

3.1. Preparatory considerations

For the first test of the proposed method reported here, hydrogen sulfide (H_2S) and methane (CH_4) were selected as the measured analyte and carrier gas, respectively, and the measurement wavelength was set to 1574 nm. The choice of CH_4 can be attributed to the widespread application of photoacoustic measurements in the oil and gas industry, where the analyzed gases can contain CH_4 up to 80 %. Therefore, while air can be used as a carrier gas in some cases, the selection of gas mixtures in photoacoustic measurement systems for industrial applications is crucial to ensure precise and reliable results. The advantages and further reasons behind these choices are given in Section 5. During the calibration phase, the amount of the noble gas mixture added to CH_4 was 75 % (see Table 1), while during the test phase, both the resonance frequency and the heat capacity were varied by adding the noble gas mixture in different total concentrations to CH_4 (see Table 2).

Complete calibrations were executed in the test phase, because in this way the accuracy of the proposed method can be justified not only by comparing the estimated and actual concentrations but also by comparing the estimated and actual sensitivities. Similarly to the calibration phase, the compositions of the test gas are kept as simple as possible by using mixtures of CH_4, helium (He) and argon (Ar) without maintaining the sum of noble gas concentrations at a constant value.

3.2. The experimental setup

Fig. 3 shows the schematics of the measurement setup used both for the calibration and the test of the proposed method. The light source of our PA system is a distributed-feedback diode laser (FITEL FRL15DCWD-A82-19030) with an emitted light power of 40 mW operated at the wavelength of 1574 nm. The diode laser is tuned to the top of the selected absorption line by adjusting its temperature, while its wavelength is modulated by superimposing a sinusoidal current modulation (1f) with an amplitude of 8 mA on an unmodulated current of 192 mA. The PA cell is a longitudinal differential cell made of stainless steel, containing two 40 mm long resonator tubes with an inner diameter of 3.5 mm each. The PA signal is detected by the microphones (Knowles EK-23029–000) placed at the centre of the resonator tubes, where the amplitude of the acoustic standing wave has its peak value. The PA system was operated at room temperature (typically 22 ± 2 °C). Nevertheless, the temperature sensitive components of the system were temperature stabilized, thus the detecting unit (i.e. the photoacoustic cell at 40 ± 0.5 °C) and the diode laser (17.81 ± 0.01 °C) were temperature controlled. The detected microphone signal is processed by an electronic control unit, which has an amplification factor of 6000. In this paper the numerical value of the PA signal is given as the microphone signal before electrical amplification. The electronics calculates the PA signal from the amplified and time-averaged microphone signal by using the digital lock-in detection technique. The sampling frequency is 16 times the modulation frequency while the PA signal averaging time

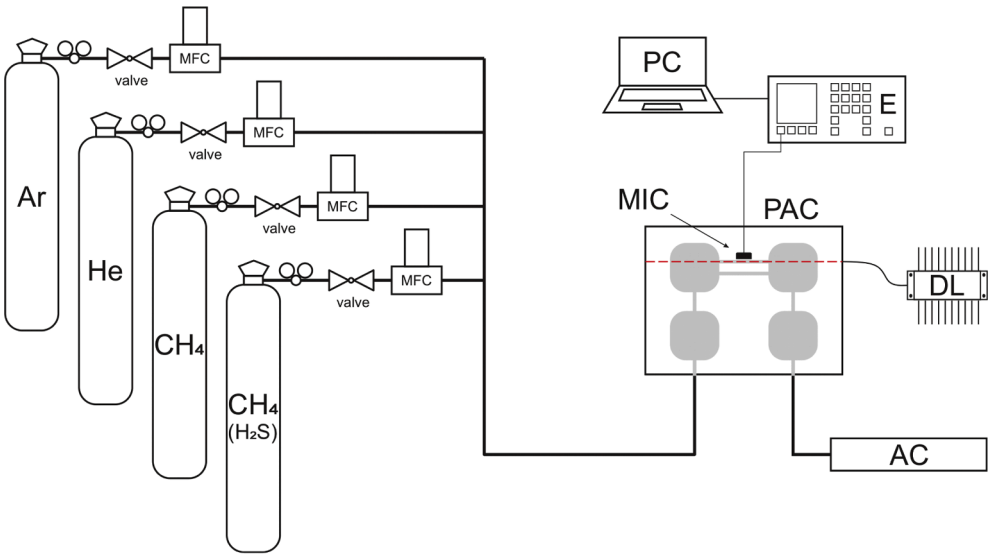

Fig. 3. Schematics of the experimental arrangement. The PA detection unit contains a PA cell (PAC), a diode laser (DL), a microphone (MIC), a controlling and signal processing electronic unit (E), and a computer (PC). The gas handling system incorporates four mass-flow controllers (MFC) and an absorber cell (AC) filled with zinc oxide.

varies from 35.2 s (@ $f = 4421$ Hz) to 60.3 s (@ $f = 7863$ Hz).

The gas handling unit includes four gas cylinders (supplied by Messer Hungarogas Ltd.): three of them contain pure He, Ar and CH_4 (each gas has a purity of 5.0), and one contains 10,000 (±200) ppm of H_2S buffered in CH_4. All measurements are performed at atmospheric pressure. Mass flow controllers (Brooks 5850 s, Brooks Instruments) are used to control the gas flows in a way that the total volumetric flow rate through the PA cell is about 200 sccm ($cm^3 \cdot min^{-1}$). Although the actual value of the total volumetric flow rate does not affect the accuracy of the reported measurements, the ratio of the individual rates is a critical parameter of the calibration measurements; therefore, an absolute flow metre (Defender 530+, Mesa Labs) with an accuracy of about 2 % is used to calibrate the flow controllers before the PA measurements and to verify the validity of this calibration after the completion of the measurements, too. For safety and environmental reasons, a H_2S absorber filled with zinc oxide (ZnO) is placed after the PA cell.

3.3. Gas sample generation

Concentration variations were generated by stepwise replacement of the flow of pure CH_4 with a flow from the cylinder that contained both CH_4 and H_2S by ensuring a constant total CH_4 concentration. Depending on the flow ratio of pure and H_2S enriched CH_4, the H_2S concentrations took five values (zero plus four others). Tables 1 and 2 list the gas compositions used during the calibration and the test, respectively. They also contain the calculated (γ-1) values and the measured and calculated resonance frequencies.

4. Results

The sensitivities determined during the execution of the proposed calibration method and during its test can be seen in Fig. 4. Squares represent the sensitivity values determined at selected frequencies during calibration (S_c (f_c)), and the solid line indicates the interpolated sensitivity curve (S_c (f)) fitted on S_c (f_c) values. The circles represent sensitivities determined during the test of the method. Similarly, in Fig. 5 the squares, the solid line, and the circles represent the FWHM values determined at selected frequencies during calibration (Δf_c (f_c)), the interpolation curve (Δf_c (f)) fitted on Δf_c (f_c) values, and the FWHM values determined during the testing of the method (Δf_a (f_a)), respectively. In Figs. 4 and 5 the S_d (f_a) and Δf_a (f_a) values, respectively are

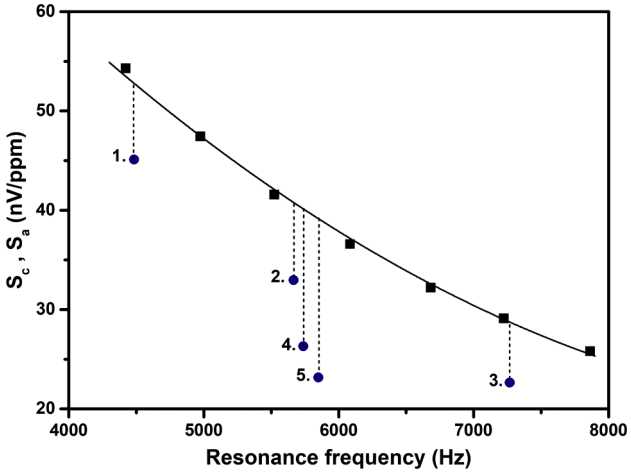

Fig. 4. Sensitivities of the PA system at different gas compositions plotted against the resonance frequency corresponding to the given gas composition. Black squares and blue circles represent sensitivities determined during calibration (S_c (f_c)) and testing (S_a (f_a)), respectively, while the solid the line is the interpolated sensitivity curve (S_c (f)) fitted on S_c (f_c) values. Legends correspond to the sequential numbers in Table 2. Vertical dashed lines visualize the differences in sensitivities due to differences in (γ-1).

labelled by their sequential number from Table 2.

The relative deviation between the measured and derived sensitivities, as well as the measured and calculated concentrations, can be seen in Figs. 6 and 7, respectively, in the latter case as a histogram. In both Figures, sensitivities and concentrations are calculated by using Equation (3). To emphasise the importance of considering the dependencies on the heat capacity of the measured gas, Fig. 7 also shows the histogram of two simplified calculation methods (see the next Section).

5. Discussion

This section covers four topics. We discuss the reasons behind the selection of the experimental parameters for the first execution of the proposed method, we compare the accuracy with the two simplified approaches, we suggest methods that can supplement PA signal

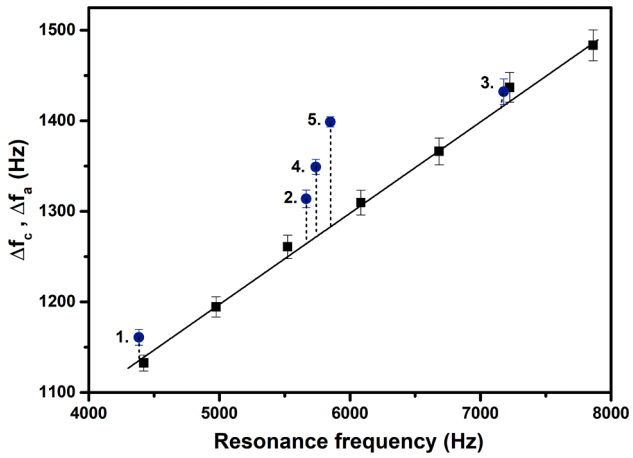

Fig. 5. FWHMs of the resonance frequency of the PA cell plotted against the resonance frequency corresponding to the given gas composition. The black squares and blue circles represent FWHMs determined during calibration (Δf_c (f_c)) and testing (Δf_a (f_a)), respectively, while the solid line is the interpolated FWHM curve (Δf_c (f)) fitted on the Δf_c (f_c) values. The legends correspond to the sequential numbers in Table 2. Vertical dashed lines visualize the differences in Δf due to differences in (γ-1).

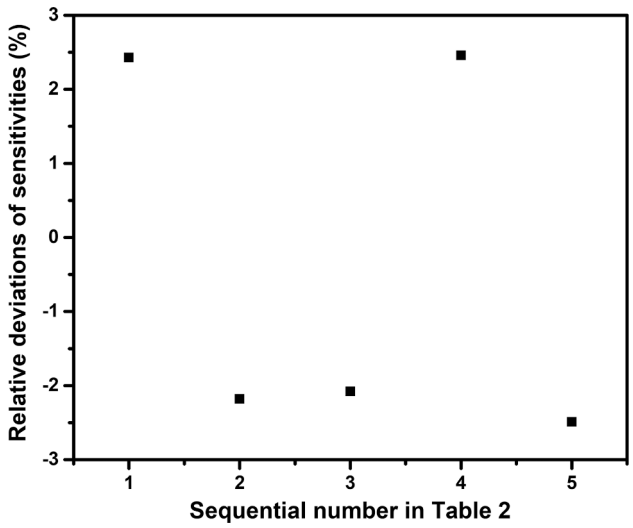

Fig. 6. Percentage relative deviations between the sensitivities measured and calculated with Equation (3) during the test phase. Sequential numbers are taken from Table 2.

measurements to determine $(\gamma\text{-}1)_a$ and Δf_a (f_a), and finally we discuss the general applicability of the suggested method.

First, selecting H_2S as the measured analyte and CH_4 as the carrier gas, for the test of the proposed method has several advantages:

- H_2S measurement in CH_4 (or in CH_4 rich gas mixtures) is both an important research topic [29,30] and one of the flagship applications of our PA systems [4].
- Due to its highly asymmetric molecular structure, H_2S has rather strong absorption lines in the near infrared, 1574 nm was selected for the measurements.
- Telecommunication type diode lasers operating in the near-infrared wavelength range have high stability both in terms of wavelength and output light power, so the constancy of the experimental parameters, other than those we varied deliberately, is ensured.
- At this measurement wavelength there is no spectral interference between these two components. Although there are wavelengths in the infrared where the influence of CH_4 on H_2S relaxation has been investigated [31], around 1574 nm the delayed relaxation of the excited state of H_2S has not been observed, and several studies for H_2S detection in the presence of CH_4 were published [4,8,24].
- Our experience shows that the influence of adsorption/desorption effects on H_2S measurements is considered negligible compared to other possible target analyte (including water vapour or ammonia).

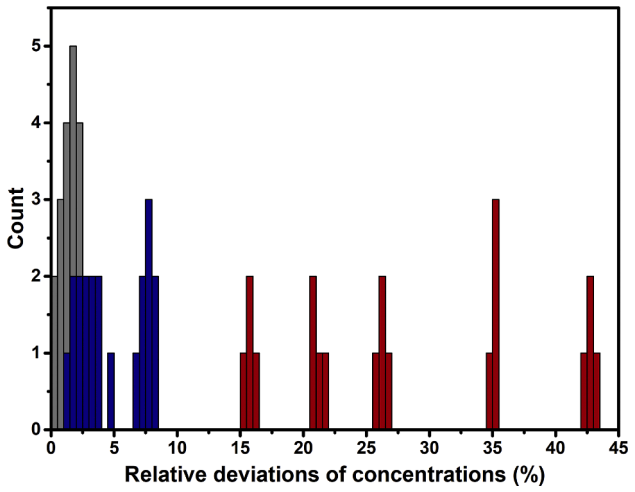

Fig. 7. Rectangles with grey, blue and red colours represent the distribution of the absolute value of the percentage relative deviations between the actual and the calculated H_2S concentrations using the proposed (grey), a simplified (blue), and an oversimplified (red) calculation method, respectively (see text for further details).

Second, to emphasise the importance of all the investigated dependencies, the measurement accuracies of the proposed method and two simplified approaches are compared. The first reference approach is clearly erroneous (oversimplified) as it only considers the frequency dependence of S, but neglects the dependence of S and Δf on the heat capacity. This oversimplification corresponds to setting both fractions on the right side of Equation (3) to be one, i.e., assuming S_a (f_a) and S_c (f_a) to be equal. As expected, this oversimplification can lead to relative errors in concentration determination up to 50 % (see Fig. 7). The second simplified reference approach counts with the frequency dependence of S and its direct proportionality to (γ-1) as well, but falsely disregards the relationship between Δf and (γ-1), i.e., the last fraction on the right side of Equation (3) is set to be one by assuming its numerator and denominator to be equal. In other words, this simplification leads to the following approximation of the actual sensitivity:

$$S_a(f_a) \approx S_c(f_a) \cdot \frac{(\gamma-1)_a}{(\gamma-1)_c} \tag{8}$$

While this simplification is clearly erroneous, Fig. 7 shows that the accuracy (up to 10 %) is considerably better than the one achieved with the oversimplified approach. We note that in certain applications where no low percentage accuracy is required, this simplified approach might be used (although not at all recommended). Table 3 compares the three methods.

Third, the demonstrated percentage level of relative accuracy can be achieved in actual measurement situations whenever the operation of the PA system includes methods for the accurate measurement of (γ-1) and Δf_a. The former quantity can be either measured directly by using sensors [21] that supplement the PA system, or can be calculated from the measured concentrations of the main components of the gas mixture [28]. As far as Δf_a is concerned, its actual value can be deduced in parallel with the determination of the actual value of the resonance frequency (f_a), a parameter that must be measured continuously in any

Table 3
Comparison of the proposed method with a simplified and an erroneously oversimplified approach.

PHASES OF OPERATION	FEATURES	PROPOSED METHOD	SIMPLIFIED APPROACH	OVERSIMPLIFIED APPROACH
CALIBRATION	Restrictions	Gas mixtures with constant heat capacity must be used	No restriction on heat capacity of the calibration gases	No restriction on heat capacity of the calibration gases
	Frequency dependence of the sensitivity	Considered	Considered	Considered
	(γ-1) dependence of the sensitivity	Considered	Considered	Not considered
	(γ-1) dependence of the resonance FWHM	Considered	Not considered	Not considered
CONCENTRATION CALCULATION	Supplementary measurements	1. Heat capacity 2. Resonance FWHM	Heat capacity	–
	Calculation of the actual sensitivity	By using Equation (3) (correction of the frequency dependent sensitivity with the actual value of Δf and (γ-1))	Correction of the frequency dependent sensitivity with the actual value of (γ-1)	The frequency dependent sensitivity is not corrected
	Relative accuracy of the concentration determination	A few percent	Up to ten percent	Several tens of percent

case. For the simultaneous determination of f_a and Δf_a, one can apply the "chirp" method [12] or, whenever the variation in the material properties of the measured gas is slow (i.e., it happens on the time scale of minutes or hours), the resonance frequency can be recorded by scanning the laser modulation frequency step by step.

Finally, regarding the general applicability of the proposed method for more complex gas mixtures that may exhibit spectral interferences and/or delayed molecular relaxation effects the following consideration has been made. Since the spectral interference appearing in Equation (1) as an additional and constant term which cannot influence the S_a (f_a) value in Equation (3), the applicability of the method into the PA system's operational algorithm seems feasible even in this case. For the investigation of the effect of molecular relaxation of the proposed method, more extended and systematic measurement series are deemed essential which is beyond the scope of this study. Therefore, the molecular relaxation is a possible limitation for the general applicability of the proposed method. Overall, the proposed method opens-up novel possibility for significant increase the accuracy of the PA system when the actual concentrations of the measured gas mixtures are known.

6. Summary and conclusions

This paper reports the first execution of a novel method which proved to ensure percentage level relative accuracy of PA concentration measurements even under varying gas composition. The reported results prove that while it is not sufficient to consider the well-known dependencies of the PA system's sensitivity: i.e., its frequency dependence and its direct proportionality on (γ-1) only, percentage level relative accuracy can only be achieved by considering the $\Delta f - (\gamma\text{-}1)$ relationships too. Although the simplified approach can lead to relative errors in the concentration calculation up to 10 %, by considering all the dependencies 1 % relative accuracy can be achieved. To this end, we propose a special calibration and concentration calculation method that has been successfully tested. The specialty of the calibration is that while it varies the resonance frequency of the PA cell, it keeps the heat capacity of the calibration gases at a constant value.

Concerning the general applicability of the proposed method for more complex gas mixtures –that may exhibit spectral interferences and/or delayed molecular relaxation effects too – the integration of the method into the PA system's operational algorithm seems feasible. Therefore, this technique is expected to become a standard and indispensable component of PA systems measuring gas or aerosol concentrations under varying gas compositions.

Declaration of competing interest

The authors declare that they have no known competing financial interests or personal relationships that could have appeared to influence the work reported in this paper.

Data availability

Data will be made available on request.

Acknowledgements:

The work was supported by the National Research, Development and Innovation Office (NKFIH), project numbers: OTKA-K-138176 and 2018-2.1.3-EUREKA-2018-00026.

References

[1] Z. Bozóki, M. Szakáll, A. Mohácsi, G. Szabó, Z. Bor, Diode laser based photoacoustic humidity sensors, Sens. Actuators B Chem. 91 (2003) 219–226, https://doi.org/10.1016/S0925-4005(03)00120-5.
[2] P. Varga, N. Vida, P. Hartmann, A. Szabó, Á. Mohácsi, G. Szabó, M. Boros, E. Tuboly, Alternative methanogenesis - Methanogenic potential of organosulfur administration, PLoS ONE. 15 (2020), https://doi.org/10.1371/journal.pone.0236578.
[3] L.G. Silva, S.C.E. Bueno, M.G. da Silva, L. Mota, M.S. Sthel, M.P.P. de Castro, R. M. Santiago Neto, V.M. Kuba, Photoacoustic detection of ammonia exhaled by individuals with chronic kidney disease, Lasers Med. Sci. 37 (2022) 983–991, https://doi.org/10.1007/s10103-021-03342-w.
[4] A. Varga, Z. Bozóki, M. Szakáll, G. Szabó, Photoacoustic system for on-line process monitoring of hydrogen sulfide (H2S) concentration in natural gas streams, Appl. Phys. B Lasers Opt. 85 (2006) 315–321, https://doi.org/10.1007/s00340-006-2388-6.
[5] X. Yin, Y. Su, T. Xi, B. Chen, L. Zhang, X. Zhang, L. Liu, X. Shao, Research progress on photoacoustic SF_6 decomposition gas sensor in gas-insulated switchgear, J. Appl. Phys. 131 (2022) 130701, https://doi.org/10.1063/5.0089426.
[6] M. Szakáll, Á. Mohácsi, D. Tátrai, A. Szabó, H. Huszár, T. Ajtai, G. Szabó, Z. Bozóki, Twenty Years of Airborne Water Vapor and Total Water Measurements of a Diode Laser Based Photoacoustic Instruments, Front. Phys. 8 (2020), https://doi.org/10.3389/fphy.2020.00384.
[7] G. Wu, Z. Gong, J. Ma, H. Li, M. Guo, K. Chen, W. Peng, Q. Yu, L. Mei, High-sensitivity miniature dual-resonance photoacoustic sensor based on silicon cantilever beam for trace gas sensing, Photoacoustics. 27 (2022) 100386, https://doi.org/10.1016/j.pacs.2022.100386.
[8] G. Wu, Z. Gong, H. Li, J. Ma, K. Chen, W. Peng, Q. Yu, L. Mei, High-Sensitivity Multitrace Gas Simultaneous Detection Based on an All-Optical Miniaturized Photoacoustic Sensor, Anal. Chem. 94 (2022) 12507–12513, https://doi.org/10.1021/acs.analchem.2c02767.
[9] Z. Bozóki, A. Pogány, G. Szabó, Photoacoustic instruments for practical applications: Present, potentials, and future challenges, Appl. Spectrosc. Rev. 46 (2011) 1–37, https://doi.org/10.1080/05704928.2010.520178.
[10] A. Fathy, Y.M. Sabry, I.W. Hunter, D. Khalil, T. Bourouina, Direct Absorption and Photoacoustic Spectroscopy for Gas Sensing and Analysis: A Critical Review, Laser Photonics Rev. 16 (2022) 2100556, https://doi.org/10.1002/lpor.202100556.

[11] D. Tátrai, Z. Bozóki, G. Szabó, Method for wavelength locking of tunable diode lasers based on photoacoustic spectroscopy, Opt. Eng. 52 (2013), https://doi.org/10.1117/1.OE.52.9.096104.
[12] M. Szakáll, A. Varga, A. Pogány, Z. Bozóki, G. Szabó, Novel resonance profiling and tracking method for photoacoustic measurements, Appl. Phys. B Lasers Opt. 94 (2009) 691–698, https://doi.org/10.1007/s00340-009-3391-5.
[13] M. Szakáll, H. Huszár, Z. Bozóki, G. Szabó, On the pressure dependent sensitivity of a photoacoustic water vapor detector using active laser modulation control, Infrared Phys. Technol. 48 (2006) 192–201, https://doi.org/10.1016/j.infrared.2006.01.002.
[14] M. Szakáll, J. Csikós, Z. Bozóki, G. Szabó, On the temperature dependent characteristics of a photoacoustic water vapor detector for airborne application, Infrared Phys. Technol. 51 (2007) 113–121, https://doi.org/10.1016/j.infrared.2007.04.001.
[15] M. González, G. Santiago, V. Slezak, A. Peuriot, Novel optical method for background reduction in resonant photoacoustics, Rev. Sci. Instrum. 78 (2007) 084903, https://doi.org/10.1063/1.2778624.
[16] M. Müller, T. Rück, S. Jobst, J. Pangerl, S. Weigl, R. Bierl, F.-M. Matysik, An Algorithmic Approach to Compute the Effect of Non-Radiative Relaxation Processes in Photoacoustic Spectroscopy, Photoacoustics. 26 (2022) 100371, https://doi.org/10.1016/j.pacs.2022.100371.
[17] J. Hayden, B. Baumgartner, B. Lendl, Anomalous Humidity Dependence in Photoacoustic Spectroscopy of CO Explained by Kinetic Cooling, Appl. Sci. 10 (2020) 843, https://doi.org/10.3390/app10030843.
[18] A. Zifarelli, M. Giglio, G. Menduni, A. Sampaolo, P. Patimisco, V.M.N. Passaro, H. Wu, L. Dong, V. Spagnolo, Partial Least-Squares Regression as a Tool to Retrieve Gas Concentrations in Mixtures Detected Using Quartz-Enhanced Photoacoustic Spectroscopy, Anal. Chem. 92 (2020) 11035–11043, https://doi.org/10.1021/acs.analchem.0c00075.
[19] P.M. Morse, K.U. Ingard, Theoretical acoustics, Princeton University Press, Princeton, N.J., 1986.
[20] V. Hanyecz, A. Mohácsi, A. Pogány, A. Varga, Z. Bozóki, I. Kovács, G. Szabó, Multi-component photoacoustic gas analyzer for industrial applications, Vib. Spectrosc. 52 (2010) 63–68, https://doi.org/10.1016/j.vibspec.2009.10.004.
[21] I. Marić, A procedure for the calculation of the natural gas molar heat capacity, the isentropic exponent, and the Joule-Thomson coefficient, Flow Meas. Instrum. 18 (2007) 18–26, https://doi.org/10.1016/j.flowmeasinst.2006.12.001.
[22] A.L. Balogh, F. Petak, G.H. Fodor, J. Tolnai, Z. Csorba, B. Babik, Capnogram slope and ventilation dead space parameters: comparison of mainstream and sidestream techniques, Br. J. Anaesth. 117 (2016) 109–117, https://doi.org/10.1093/bja/aew127.
[23] R.H. Vafaie, R. Shafiei pour, S. Nojavan, K. Jermsittiparsert, Designing a miniaturized photoacoustic sensor for detecting hydrogen gas, Int. J. Hydrog. Energy. 45 (2020) 21148–21156, https://doi.org/10.1016/j.ijhydene.2020.05.261.
[24] A. Szabó, Á. Mohácsi, G. Gulyás, Z. Bozóki, G. Szabó, In situ and wide range quantification of hydrogen sulfide in industrial gases by means of photoacoustic spectroscopy, Meas. Sci. Technol. 24 (2013), https://doi.org/10.1088/0957-0233/24/6/065501.
[25] J.-P. Besson, S. Schilt, L. Thévenaz, Multi-gas sensing based on photoacoustic spectroscopy using tunable laser diodes, Spectrochim. Acta. A. Mol. Biomol, Spectrosc. 60 (2004) 3449–3456, https://doi.org/10.1016/j.saa.2003.11.046.
[26] T. Rück, M. Müller, S. Jobst, S. Weigl, J. Pangerl, R. Bierl, F.-M. Matysik, Digital Twin of a photoacoustic trace gas sensor for monitoring methane in complex gas compositions, Sens. Actuators B Chem. 378 (2023) 133119, https://doi.org/10.1016/j.snb.2022.133119.
[27] M. Guo, X. Zhao, K. Chen, D. Cui, G. Zhang, C. Li, Z. Gong, Q. Yu, Multi-mechanism collaboration enhanced photoacoustic analyzer for trace H2S detection, Photoacoustics. 29 (2023) 100449, https://doi.org/10.1016/j.pacs.2023.100449.
[28] A. Burcat, B. Ruscic, Chemistry, Third Millenium Ideal Gas and Condensed Phase Thermochemical Database for Combustion (with Update from Active Thermochemical Tables) (2005), https://doi.org/10.2172/925269.
[29] X. Yin, L. Dong, H. Wu, W. Ma, L. Zhang, W. Yin, L. Xiao, S. Jia, F.K. Tittel, Ppb-level H_2S detection for SF_6 decomposition based on a fiber-amplified telecommunication diode laser and a background-gas-induced high- Q photoacoustic cell, Appl. Phys. Lett. 111 (2017) 031109, https://doi.org/10.1063/1.4987008.
[30] X. Tian, G. Cheng, Y. Cao, J. Chen, K. Liu, X. Gao, Simultaneous detection of hydrogen sulfide and carbon dioxide based on off-axis integrated cavity output spectroscopy using a near-infrared distributed feedback diode laser, Microw. Opt. Technol. Lett. 63 (2021) 2074–2078, https://doi.org/10.1002/mop.32887.
[31] M. Olivieri, G. Menduni, M. Giglio, A. Sampaolo, P. Patimisco, H. Wu, L. Dong, V. Spagnolo, Characterization of H2S QEPAS detection in methane-based gas leaks dispersed into environment, Photoacoustics. 29 (2023) 100438, https://doi.org/10.1016/j.pacs.2022.100438.

Panna Végh (born in 1997) is a PhD student at the University of Szeged. She began her graduate studies in 2015 and achieved MSc degree in physics in 2020. Her current research interests include investigation of the process of photoacoustic signal generation and determination of the sensitivity of photoacoustic systems.

Gábor Gulyás, researcher at University of Szeged since 2019. He received his MSc in Physics at University of Szeged in 2010. He was working as a development engineer at Hilase Ltd. between 2010 and 2016 developing photoacoustic spectroscopy based gas analysers for natural gas industry and environmental monitoring.

Helga Huszár is a research fellow at the Photoacoustic Research Group at Department of Optics and Quantum Electronics, Szeged, Hungary, from 2019. She received her MS degree in physics and PhD degrees in environmental sciences from the University of Szeged, Hungary, in 2003 and 2009. Since 2007 to 2019 she had been working as a development engineer at Hilase Ltd and Hobre Laser Technology Ltd. Her current research interests include photoacoustic spectroscopy and its application in industrial measurements and atmospheric trace gas detection.

Tibor Ajtai, Head of Laser and Aerosol Research Laboratory (LARLab), senior research fellow at University of Szeged. He received his PhD in Physics at University of Szeged in 2012. His main research areas are: ambient aerosol research, generation and characterisation of nanoaerosols, emission based fuel development.

Gábor Szabó is a full member of the Hungarian Academy of Sciences since 2010 and the Head of the Physics Doctoral School at University of Szeged since 2007. He has been working at the University of Szeged from 1978 to present, since 1994 as a professor. Since 2020 he is the Managing Director of ELI-ALPS. His research fields and interests include photoacoustic spectroscopy, ultrafast laser spectroscopy, generation of femtosecond pulses, nonlinear optics, control of quantum systems and applications of lasers in medicine.

Anna Szabó received her MSc and PhD degrees in physics in 2010 and 2016, respectively. She has been working at University of Szeged from 2013 to present. Since 2022 she is a research fellow of the ELKH-SZTE Research Group for Photoacoustic Monitoring of Environmental Processes. Her research interest includes photoacoustic spectroscopy based gas analysis for medical research and environmental monitoring.

Zoltán Bozóki received his MSc, PhD and DSc degrees in physics in 1989, 1997 and 2012, respectively. He has been working at the University of Szeged from 1994 to present, since 2013 as a professor. Since 2022 he is the principal investigator of the ELKH-SZTE Research Group for Photoacoustic Monitoring of Environmental Processes. He has been participated in the development and successful commercialisation of photoacoustic instruments for various applications including oil and gas industry and environmental monitoring. For his innovations in the field of photoacoustics he has received various prices including the Gábor Dénes Award in 2017.